STRENGTHENING OF STEEL AND CONCRETE COMPOSITE TRUSSES BY UNBONDED EXTERNAL PRESTRESSING

Kanokpat Chanvaivit[1], Ekasit Limsuwan[2], and John Dawe[3]

[1] Department of Structural Engineering, Chulalongkorn University, Bangkok, Thailand
[2]Department of Structural Engineering, Chulalongkorn University, Bangkok, Thailand
[3] Department of Civil Engineering, University of New Brunswick, New Brunswick, Canada

Received Date: December 24, 2012

Abstract

In this paper, the method of strengthening of steel and concrete composite trusses by using unbonded external prestressing was presented. Based on the experimental results compared with the analytical calculations, the structures are believed to perform better than the conventional composite trusses. The additional unbonded mono-strand external prestressing tendon of 7.9% of the tension bottom chord cross sectional area results in the 20% higher load carrying capacity. Moreover, there is the advantage of the additional prestressing to improve the accuracy of the flexural stiffness determination by using the transformed section method for the truss-like structural system. However, to maintain the ductile failure mode, the amount of the strengthening tendon should be limited for the required rotational capacity. In conclusion, this method can be useful in the upgrading of the existing composite trusses for both the flexural strength and serviceability.

Keywords: Composite truss, Concrete deck slab, Experimental study, Mono-strand, Post-tensioning, prestressing, Strengthening, Steel structures, Steel truss, Tendon

Introduction

The composite action between the steel trusses and the concrete deck slab can be achieved by using the shear stud connectors welded to the top chord of the steel truss and embedded in the concrete slab as refer to ASCE Task Committee (1996) AISC (2010) and ASCE-ACI Joint Committee (1960). The method of strengthening of steel and concrete composite trusses by using external post-tensioning is introduced in this paper. The high strength tendons provide the pre-opposite stresses to the truss members prior to the service load stresses. This pre-opposite stresses lead to the additional flexural and shear capacity of the composite truss. The conventional method to design the shear stud connection for the concrete deck is still applicable by considering the higher interface shear force due to the post-tensioning; Kim, Jung and Ahn (2011), Lam and El-Lobody (2005), Nie, Xiao and Tan (2004) and Klingner et al (1982). An example of the post-tensioned composite truss was illustrated in Figure 1.

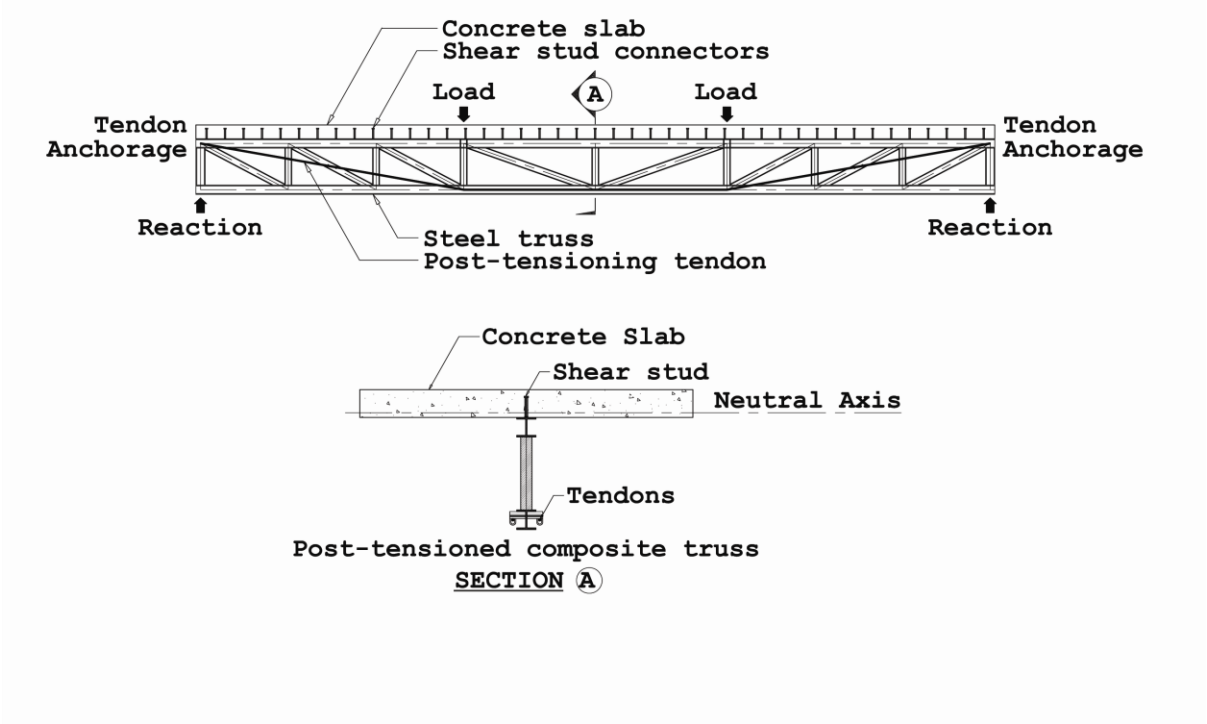

Figure 1. Example of post-tensioned composite truss

From Figure 1, suppose that in addition to the weight of the truss and slab, the structure was subjected to point loads applied at the one-third point and also at two-third point along the span length. The tendons were anchored at both far ends of the top chord and were draped down at the third points along the lower tension bottom chord to provide the opposite bending moment to the applied loads. External prestressing provides the axial compression that counteracted the tensile stresses caused by the external loads at the mid span bottom chord.

Some research papers; Uy and Craine (2004), Saadatmanesh et. al (1989) and Hoadley (1963) mention the external prestressing in the case of composite beams. It was found that the purpose of prestressing a composite beam is not to overcome the tensile deficiencies of the material as in the case of prestressed concrete. They found that the installed tendons can upgrade the flexural strength and ductility of the composite beam. This is also confirmed by Ahn, Jung and Kim (2010) and Chen, Jia and Wang (2009)

However, the increase of the internal force inside the unbonded tendons due to the additional straining under the loading cannot be neglected as it will lead to the significant under estimated results in the flexural capacity as confirmed by Vechio et al. (2006) and also Lou and Xiang (2010) Non-composite trusses post-tensioned by tendons anchored at truss joints were studied; Han and Park (2005), Ohsaki et al (2006) and Ayyub et al (1990). They used superposition in two stages of analysis. They first applied the dead load and the prestressing force without considering the stiffness of the tendons. At the second stage, live load was applied considering the stiffness of the tendons to be in effect. They found that if a tendon coincides with a truss member, then only that member is affected by post-tensioned force, but if a tendon does not coincide with truss members, then most of the truss members will be affected by post-tensioning.

Research Objectives

After thoroughly reviewing the previous researches, there is no design specification nor the full scale experimental data related to the concept of strengthening composite trusses by post-tensioning. As a result, in order to study the actual behaviors, the full scale experiment research must be conducted. Thus, the objectives of this research can be concluded as follow;

- To present the experimental study of the composite truss strengthening by the post-tensioning.
- To investigate and verify the theoretical analysis by comparing with the experimental results for the strength, the stiffness and the failure modes.
- To summarize the advantages of the strengthening of the post-tensioned composite truss; the ultimate flexural strength, the ultimate shear strength and the limitations of the maximum tendon applicable.

Research Scope

The scope of this research is limited to the monotonically loaded simply support composite trusses. The concrete deck is regarded as being perfectly bonded to the steel truss so that full composite action is achieved. All truss joints were considered to be concentric with respect to member force transfer. High strength tendons contact the truss only at the two end anchor points and the two intermediate draping points. Between these points, no contact was made between the tendons and truss and therefore no direct transfer of prestressing forces occurred in those regions. The Monostrand® DYWIDAG tendons used in this study are manufactured with their own flexible lubricated sleeves to minimize friction so that the longitudinally friction can be neglected. Additionally, draping points were fabricated and lubricated so as to reduce friction. Relaxation of the prestressing tendons was not considered since the prestressing was applied immediately prior to testing. The characteristic properties of all materials were determined by testing and used in the analyses.

Experimental Study

Test Specimens

There were 4 specimens in the experimental study which are specimen A, B, C and D. All the test specimens were mounted in a self equilibrating test frame in the structural laboratory for the total span length of 8534mm. The tendons were draped at the third points along the bottom chord of the truss at 2845mm from the center of the end vertical members. The overall length of each tendon between the two wedge anchor points was 8620mm. The composite concrete deck slabs were casted on the specimen A and B only while the specimen C and D were the steel trusses without any concrete slab. There were the 2-dia.12.7mm Grade 250 post-tensioned tendons on the specimens A and D only while there was no any post-tensioned tendon on specimen B and C. The detail information for all the specimens can be found in the table 1 and in the Figure 2 below.

Table 1. The Summary of the Test Specimens

	Specimen A	Specimen B	Specimen C	Specimen D
Span length	8534mm	8534mm	8534mm	8534mm
Concrete Deck	1800x8534x150mm (f_c'=50MPa) with DB10mm @ 250# reinforcement	1800x8534x150mm (f_c'=50MPa) with DB10mm @ 250# reinforcement	-	-
Tendon	2-dia12.7mm Grade250 DYWIDAG® Mono-strand	-	-	2-dia12.7mm Grade250 DYWIDAG® Mono-strand
Post-tensioning stress	920MPa	-	-	460MPa
Steel top chord member	W100x19 (A992)	W100x19 (A992)	W100x19 (A992)	W100x19 (A992)
Steel bottom chord member	W100x19 (A992)	W100x19 (A992)	W100x19 (A992)	W100x19 (A992)
Vertical web member	S75x8 (A992)	S75x8 (A992)	S75x8 (A992)	S75x8 (A992)
Diagonal web member	S75x8 (A992)	S75x8 (A992)	S75x8 (A992)	S75x8 (A992)
Distance between the centroid of top and bottom chord	500mm	500mm	500mm	500mm
Shear connectors	Dia.15.9mmxLong 115mm @ 150mm spacing Nelson studs	Dia.15.9mmxLong115mm @ 150mm spacing Nelson studs	-	-

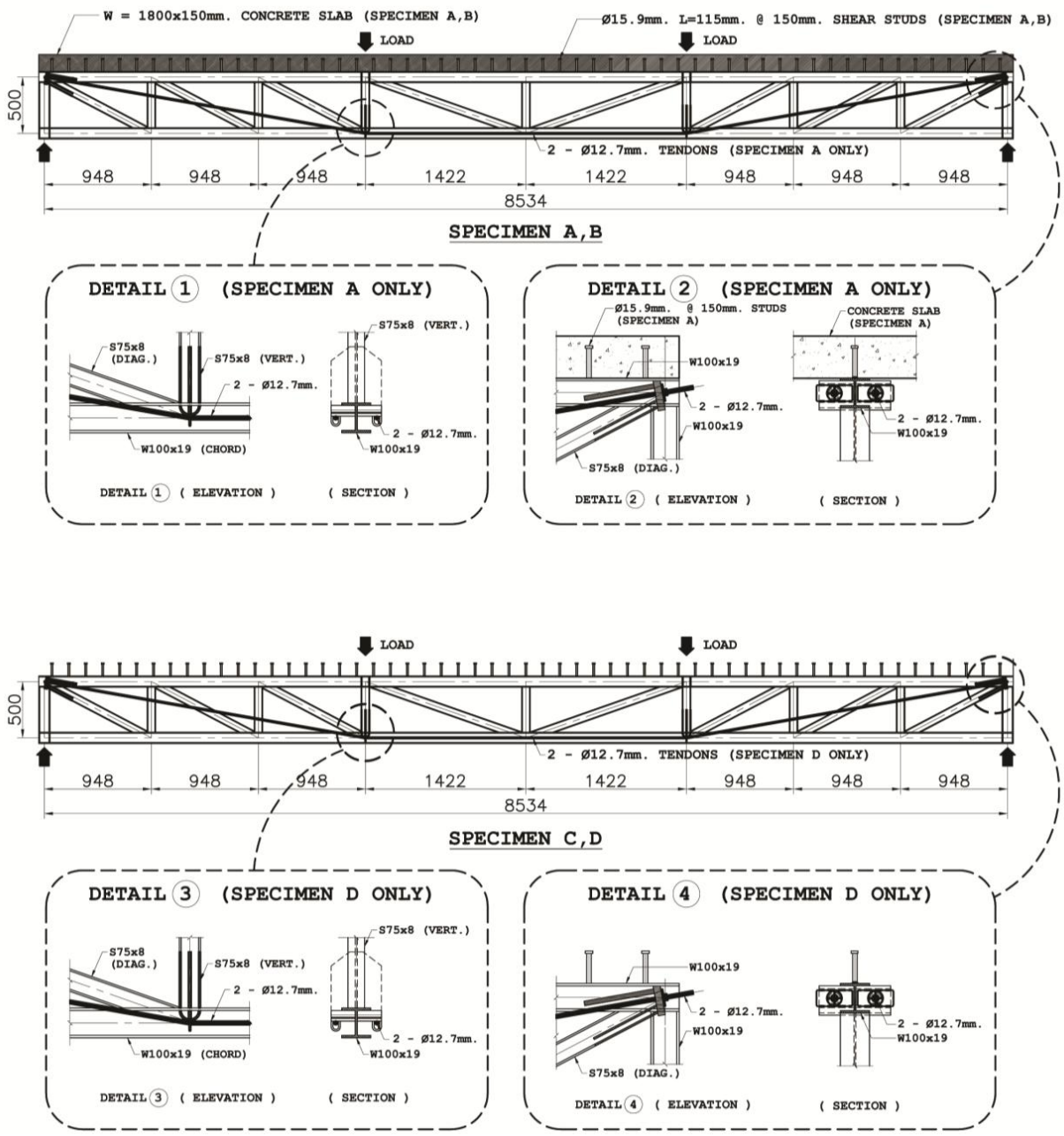

Figure 2. Test specimens

Two hydraulic twin-ram jacks and the control system from DSI America along with the pressure gauge readings were used to produce the prestressing forces. Specimens were loaded at the third points by two load rams of 1000kN capacity with a stroke of 300mm. The hydraulic hoses were connected to the two rams and hydraulic pumps. Carefully controlled the apparatus ensured that the loads applied by the two rams remained equal as indicated by the reading values from the calibrated two load cells placed between the rams and the concrete deck slab. The two pivot plates were used to adjust the angle of the load to remain perpendicular contact to the specimen at all time during the tests.

Test Materials

The specified compressive strength of the concrete mix at 28 days was 50MPa with a slump of 150mm; ACI Committee 318 (2011). The actual concrete had 2.6% air entrainment and a temperature of 15.6ºC at the time of sampling. Nine concrete cylindrical mould samples were cured under the same condition as the concrete slab. The first set of three cylinder moulds were tested for compressive strength on the 7th day after the concrete casting before the concrete forms were stripped. The detail concrete material test results are shown in the Table 2.

Table 2. Concrete Material Test Results

Concrete Age (Days)	Compressive Strength (MPa)	Actual to Design Compressive Strength Ratio	Tensile Strength (MPa)
7	47.8	0.96	-
28	55.7	1.11	-
75	62.5	1.25	5.60

The steel chord truss members were made of W100x19 sections while the vertical and diagonal web members were made of S75x8 sections, all conforming to Canadian Institute of Steel Construction (2011) and ASTM A992. The gage length used for tensile coupon testing was 49.97mm with an applied strain rate of 11.5MPa/sec conforming to the ASTM A370-03. Five samples of the 12.7mm diameter high strength tendons were subjected to tension tests to determine the ultimate tensile strength as well as the capacity of the anchorage wedge system. Tendons typically failed by rupture of the small wires one by one for a total of 7 wires. The anchorage wedges showed a capacity higher than the tendon itself. Moreover, five sample of the diameter 10mm temperature reinforcing bars were subjected to the standard tension tests. The detail steel coupons, tendons and rebar test results are shown in Table 3.

Table 3. Steel Material Test Results

Member	Average Yield Strength (MPa)	Average Yield Strain	Average Tensile Strength (MPa)	Average Tensile Strain	Tangent Modulus(MPa)
Flange W100x19	483.6	0.00237	587.3	0.2802	373.2
Web W100x19	439.7	0.00216	586.9	0.3272	452.9
Web S75x8	399.0	0.00200	503.0	0.2515	416.9
Steel Truss Members (Average)	440.7	0.00216	559.1	0.2863	416.7
Tendons (Average)	-		1715.0		-
Rebars (Average)	510.0	0.00250	860.0	-	-

Instrumentations

Regarding to the Figure 3 below, strain gages (Omega SGD-6/120-LY11 120Ω) were applied to the steel members. Strain gages (Omega KFG-30-120-C1-11L1M2R 120Ω) were used on the surface of the composite concrete deck. Deflections at mid-span and third points were measured using linear strain converters (LSCs)

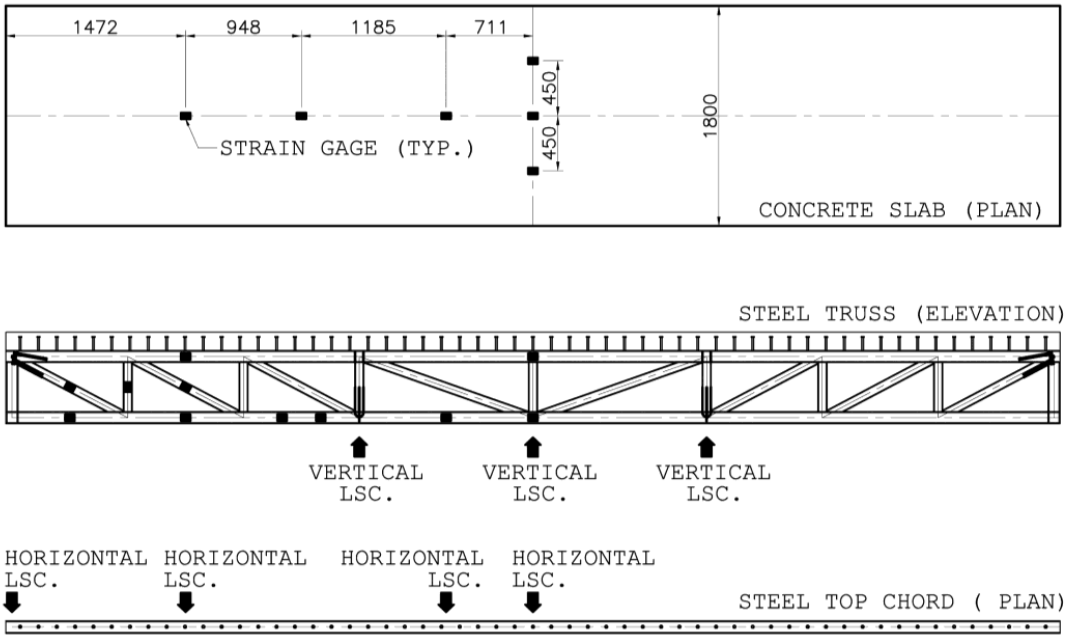

Figure 3. Locations of the instrumentations

For the lateral movement of the steel truss, LSCs were also used to detect any buckling

behavior. Each strain gage attachment point was carefully prepared according to a specified procedure. Electrical wires were soldered permanently to the strain gage terminals and connected to a Data Acquisition System (DAQ) working with the computer program LABVIEW® to display and record the data.

Test Results and Discussions

Load and Deflection Curves

After the concrete had been casted and the concrete compressive strength had reached the expected design strength, the twin-ram jacks were used to prestress the tendons. For the specimen A, the vertical loads were applied continuously up to failure by yielding of the bottom chord and simultaneous excessive deflection at mid-span as shown in the Figure 4.

Figure 4. Ultimate stage of the specimen A

For the specimen B, the two point loads were applied up to the point of ultimate which was marked by complete tensile rupture of the bottom chord as shown in Figure 5.

Figure 5. Ultimate stage of the specimen B

The steel trusses specimen C and D were basically identical to that of the specimen A and B except that there was no concrete composite slab. The specimen C was loaded with the two point loads increasing from zero up to the point of initiation of elastic buckling of the top chord as shown in Figure 6.

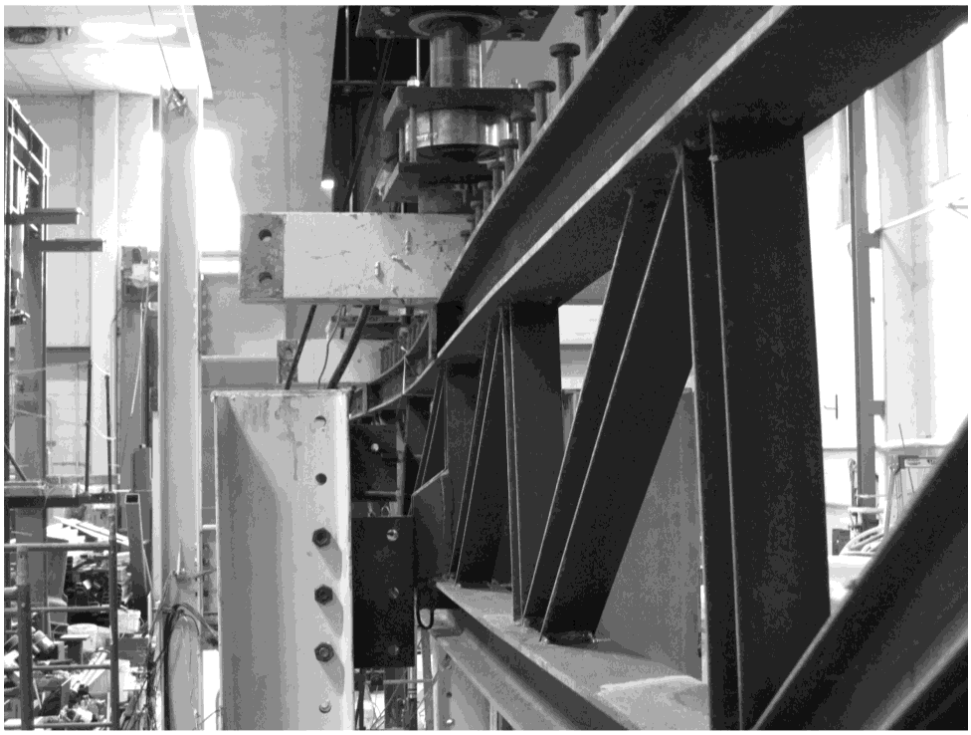

Figure 6. Ultimate stage of the specimen C

For specimen D, tendons were stressed up to 460MPa and the loads were applied up to the ultimate in the same mode as for the specimen C causing bucking in the top chord of the predicted load as shown in Figure 7.

Figure 7. Ultimate stage of the specimen D

Test results are compared with the theoretical analysis. The calculation of the load and deflection relation of the post-tensioned composite truss starts when the ram loads were applied at the third points.

The tendon force increases from initial jacking force (P) to (P+ΔP) where ΔP is the increase in tendon force due to the additional straining from the ram loads. Since this is the unbonded prestressing structure, the method of the strain compatibility only at a section is insufficient to calculate the ΔP. The strain compatibility of the whole structure must be considered. Starting with the elongation in the composite truss along the alignment of the tendons due to the vertical applied ram loads, denoted as δ1p, is then calculated from Equation (1)

$$\delta_{1p} = \left(\frac{1}{\delta P_2}\right)\sum_{i=1}^{n}\int_0^L\left(\frac{F_{i,1}(x)\delta F_{i,2}(x)}{E_i(x)A_i(x)}\right)dx \qquad (1)$$

Then the flexibility elongation coefficient, denoted as δ_{11}, which is the elongation in the composite truss along the alignment of the tendons generated by a unit load in the tendon, can be calculated from Equation (2)

$$\delta_{11} = \left(\frac{1}{\delta P_2}\right)\left\{\sum_{i=1}^{n}\int_0^L\left(\frac{F_{i,2}(x)\delta F_{i,2}(x)}{E_i(x)A_i(x)}\right)dx + \sum_{j=1}^{m}\int_0^L\left(\frac{F_{j,2}(x)\delta F_{j,2}(x)}{E_j(x)A_j(x)}\right)dx\right\} \quad (2)$$

The compatibility condition of the final relative displacement of the tendon is applied from Equation (3)

$$\delta_{11} \cdot \Delta P = \delta_{1p} \quad (3)$$

From Equation (3), the increase in tendon force due to the applied ram loads ΔP can be determined. After the internal forces in the composite truss are known, according to the equilibrium condition with the applied loads, the vertical deflection, denoted as Δ_y, due to the stresses in every parts is then can be calculated from Equation (4)

$$\Delta_y = \left(\frac{1}{\delta P_3}\right)\sum_{i=1}^{n}\int_0^L\left(\frac{F_{i,1}(x)\delta F_{i,3}(x)}{E_i(x)A_i(x)}\right)dx \quad (4)$$

The above calculation procedure is applicable for both elastic stage and the non-linear stage. For the non-linear analysis, the iteration procedure is required. After the increase in tendon internal force due to the additional straining from the ram loads (ΔP) is calculated from Equations (1), (2) and (3), all the internal forces in the truss members can then be calculated. Each of the truss members is checked. If the strain reaches the yield strain, the new value of the modulus of elasticity will be replaced as the $E_{tangent}$ in the strain hardening zone from the Table 3. The whole iterative process is then start again to find ΔP, internal forces and internal strain until one of the truss member reaches the tensile strain at the ultimate stage. The related ΔP at the ultimate stage is then used to calculated the ultimate moment capacity from Equations (5), (6), (7) and (8) explained in section 6.1

All of the symbols, notations and abbreviations are listed below;

$F_{i,1}(x)$ is the internal forces in truss member, *i*, due to the vertical applied ram loads.
$F_{i,2}(x)$ is the internal forces in truss member, *i*, due to the unit load along the tendon alignment.
$F_{i,3}(x)$ is the internal forces in truss member, *i*, due to the unit load applied vertically at mid-span.
$\delta F_{i,2}(x)$ is the virtual internal forces in truss member, *i*, due to the unit load along the tendon alignment.
$\delta F_{i,3}(x)$ is the virtual internal forces in truss member, *i*, due to the unit load applied vertically at mid-span.
$F_{j,2}(x)$ is the internal forces in tendon, *j*, due to the unit load along the tendon alignment.
$\delta F_{j,2}(x)$ is the virtual internal forces in tendon, *j*, due to the unit load along the tendon alignment.
$E_i(x)$ is the modulus of elasticity of truss member, *i*, as the function of axial strain at the iterative applied load.
$E_j(x)$ is the modulus of elasticity of tendon, *j*, as the function of axial strain at the iterative applied load.
$A_i(x)$ is the cross sectional area of truss member, *i.*
$A_j(x)$ is the cross sectional area of tendon, *j*.
δP_2 is the unit load along the tendon alignment.
δP_3 is the unit load applied vertically at mid-span.
n is the number of truss member.

m is the number of tendon.

The predicted load and deflection relations show a good agreement with the experimental results as shown in Figure 8. This is a favorable indication that the theoretical analysis adopted is valid. It is believed that the differences between the calculated values and the experimental data are primarily due to the slip of the anchorage wedges of the prestressing tendon with a loud noise during the tests.

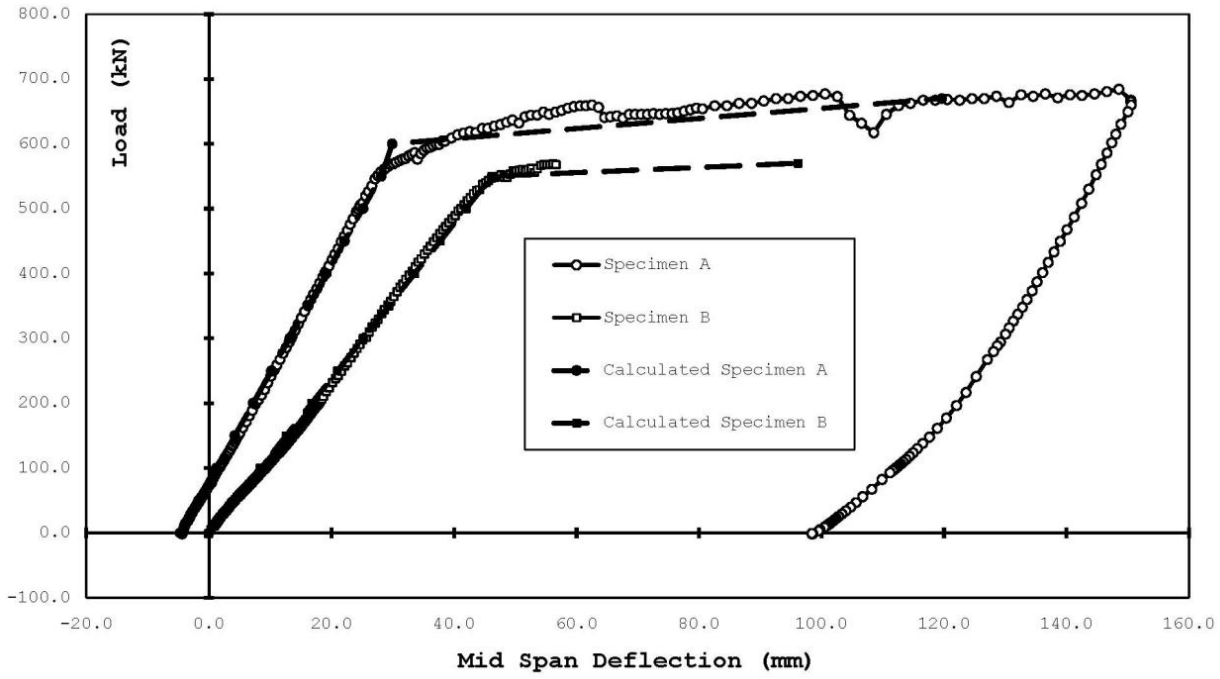

Figure 8. Load and deflection curves for specimen A and B

From Figure 8, the additional 7.9% of the cross sectional area of the post-tensioned tendons compared to the tensile bottom chord area of the truss resulted in the maximum total load of 684kN (Specimen A) which was 20.4% higher than the total load of 568kN for the case without post-tensioning. (Specimen B)

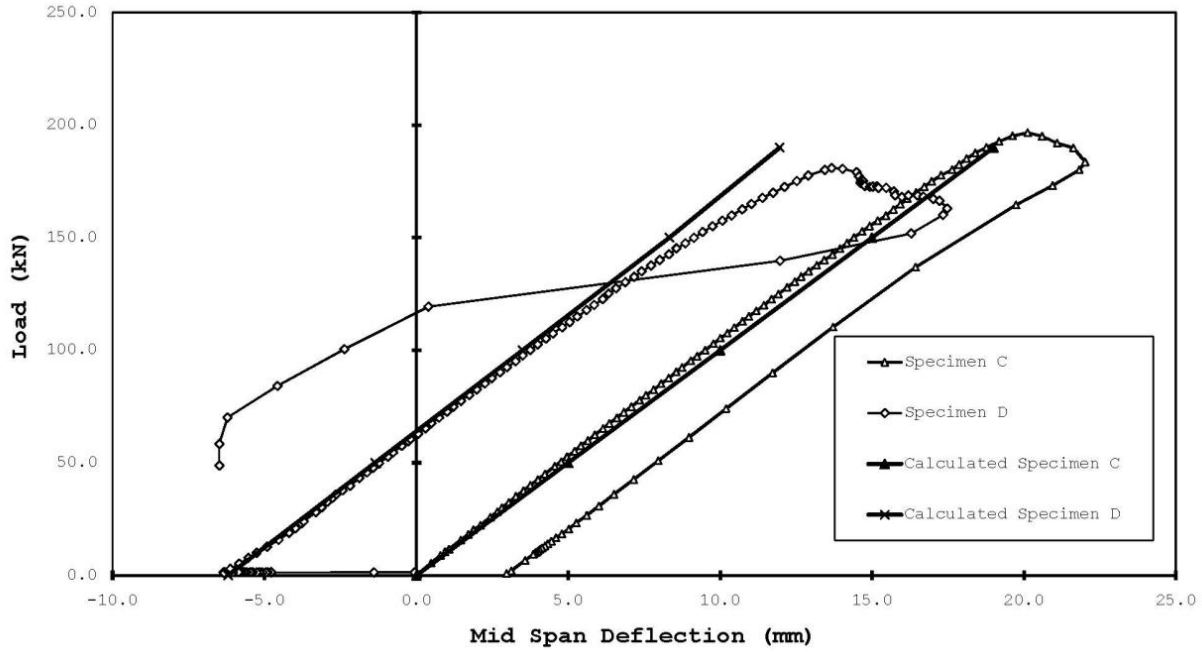

Figure 9. Load and deflection curves for specimen C and D

From Figure 9, for the Specimen D with no composite concrete deck slab, the use of post-tensioning had no advantage on the truss load carrying capacity compared to the Specimen C (without post-tensioning) because the specimen critically failed in the lateral buckling mode of the top chord.

Effect of Percentage of Tendon to the Ultimate Load Capacity

The effect of percentage of tendon to the ultimate load capacity is the major concerned of this research. In order to study this effect, variation of the percentage of post-tensioned tendon is introduced. Considering the tensile bottom chord member of post-tensioned composite truss that has a cross sectional area of $A_i(x)$ and the cross sectional area of the post-tensioned tendon, $A_j(x)$. The reinforcement ratio for the bottom chord member is then $\rho_i(x)$ and the reinforcement ratio of the post-tensioned tendon is then $\rho_j(x)$ then the total reinforcement ratio ρ_{total} equals to $\rho_i(x)+ \rho_j(x)$. The percentage of tendon, i.e. the variations of the amount of the reinforcement ratio for the bottom chord member, $\rho_i(x)$ and the total reinforcement ratio, $\rho_i(x)+ \rho_j(x)$, are plotted against the ultimate load as shown in Figure 10.

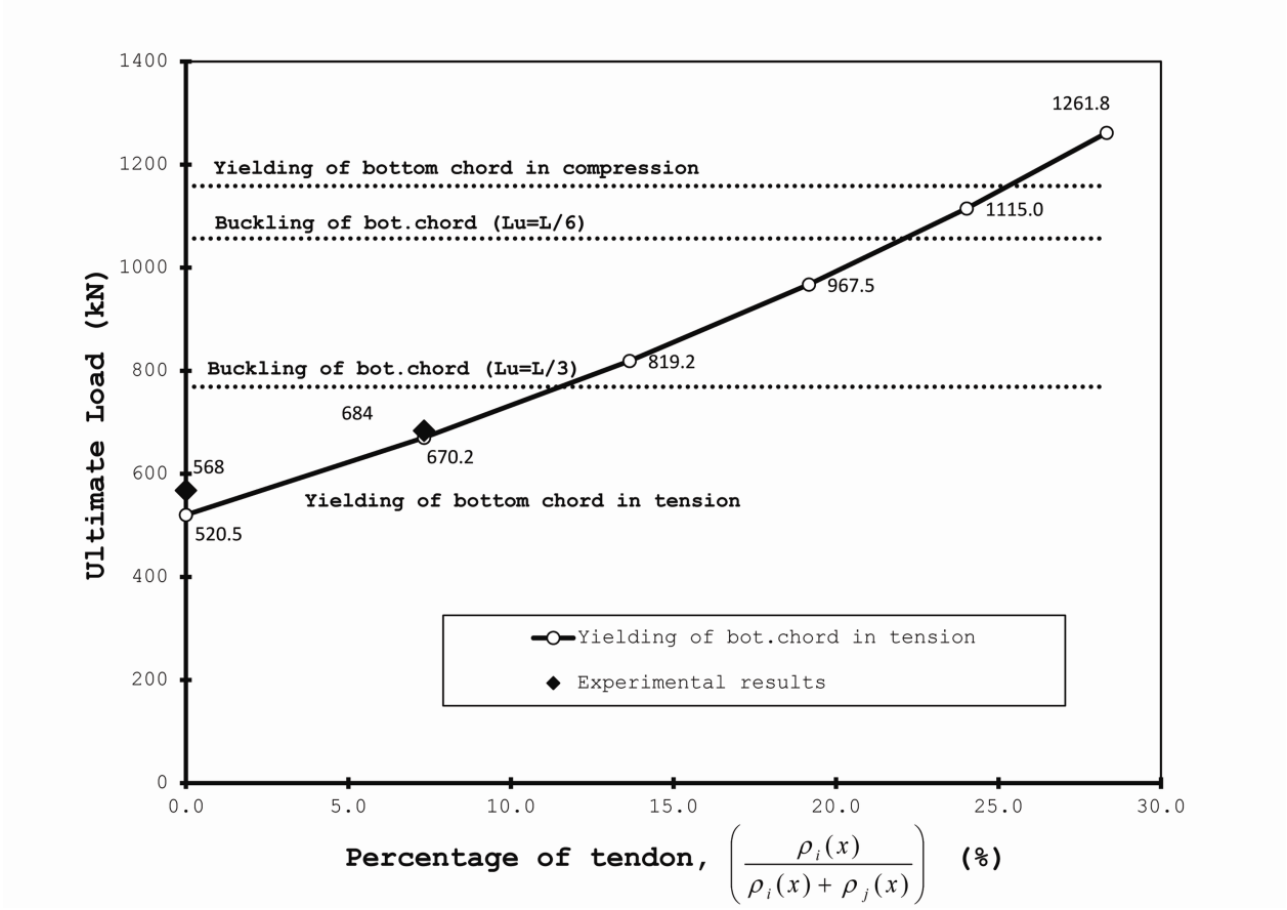

Figure 10. Effect of percentage of tendon on ultimate load capacity

From Figure 10, the effect of the percentage of tendon for various modes of failure has a significant effect on the ultimate load capacity of the structure. The additional percentage of tendon means the additional higher-strength tensile cross sectional area which leads to the advantage on the ultimate load capacity of the composite truss.

It improves the ultimate load capacity, but on the other hand, the higher percentage of the tendon can cause buckling failure of the truss bottom chord during the prestressing. The lateral bracing is an important concern when the percentage of the tendon reinforcement is increased. Lower dotted horizontal line is the limited ultimate load if the lateral bracings were provided at four locations; at each of the two supports and at two third points from both support of the truss. If the number of the lateral bracings increases to five locations; by adding the mid-span bracing, the ultimate load capacity increases to the middle dotted horizontal line. If all of the truss members are braced continuously, the ultimate load capacity will be limited by the yielding of the truss member in compression during the prestressing as shown by the upper dotted horizontal line.

Effect of Percentage of Tendon to the Rotational Capacity

The effect of the prestressing tendon on the rotational capacity of a post-tensioned composite truss is also studied in this research. In order to study this effect, the percentage of tendon are plotted against the rotational capacity as shown in Figure 11.

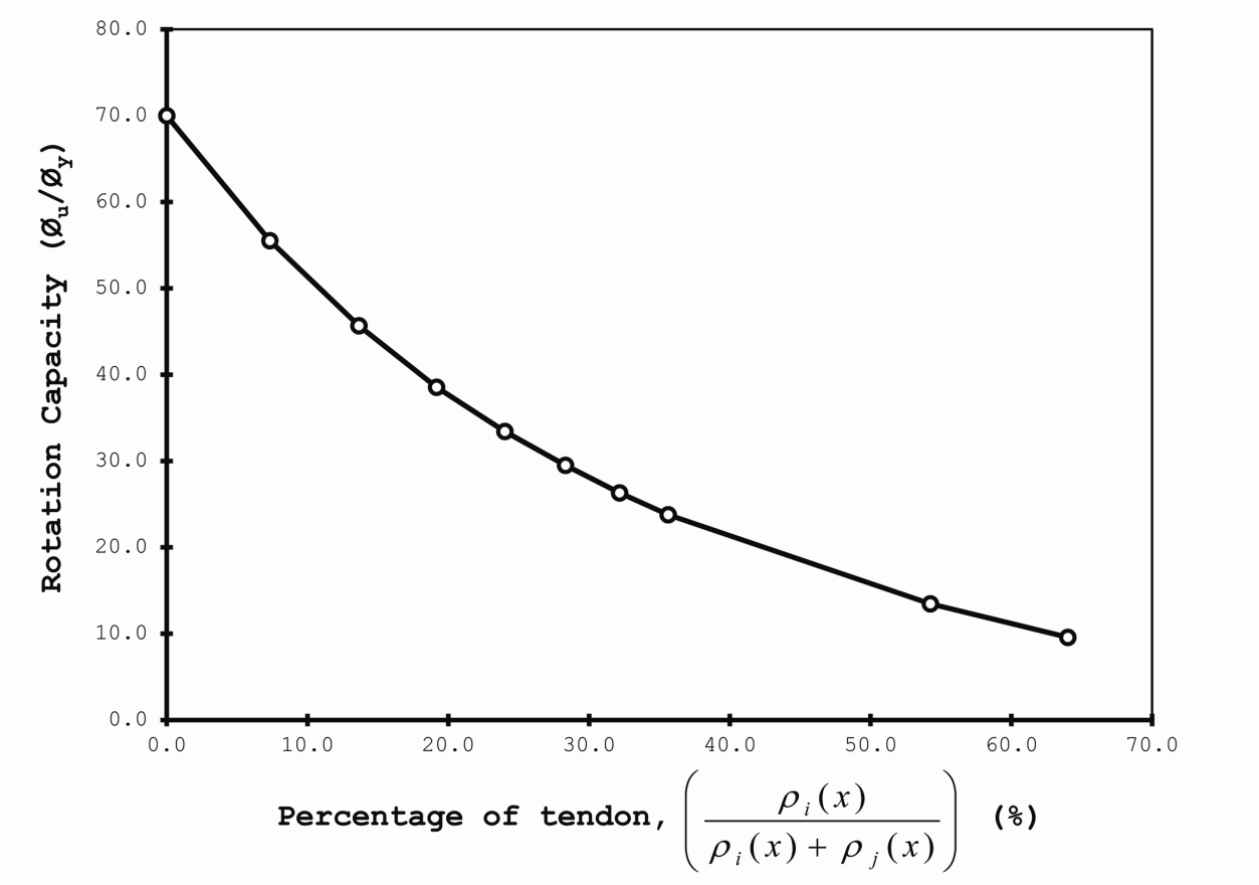

Figure 11. Effect of percentage of tendon on the rotational capacity

From Figure 11, the amount of the strengthening tendon affects the rotational capacity. It reduces the ratio of the ultimate curvature ($Ø_u$) to the yield curvature ($Ø_y$). To maintain the ductile failure mode, this relation can be utilized to achieve the required rotational capacity of the post-tensioned composite truss for the design purpose. By given the top surface concrete strain equals to the crushing strain and the tensile stress in the bottom chord and the tendons equals to the ultimate strength, the actual neutral axis in which the summation of the concrete compression equals to the total tension from the bottom chord and the tendon can be determined. The curvature at the ultimate stage then can be calculated from the top surface concrete strain divided by the distance from the top concrete surface to the neutral axis.

Effect of Percentage of Tendon to the Effective Moment of Inertia

Regarding the nature of the stiffness of the truss system compared to the beam-system, the determination of the flexural stiffness of the composite truss from the transformed section method, I_{transf}, always gives the higher stiffness value than the observed effective experimental results. The effective flexural stiffness, I_{eff}, for the truss system is approximately 60%-80% of the I_{transf}.; Samuelson (2002) and Brattland et al (1986) However, from the experimental results as well as the theoretical analysis, the percentage of tendon affects the effective flexural stiffness of the composite truss as shown in Figure 12. It improves the linearity of the load and deflection relations.

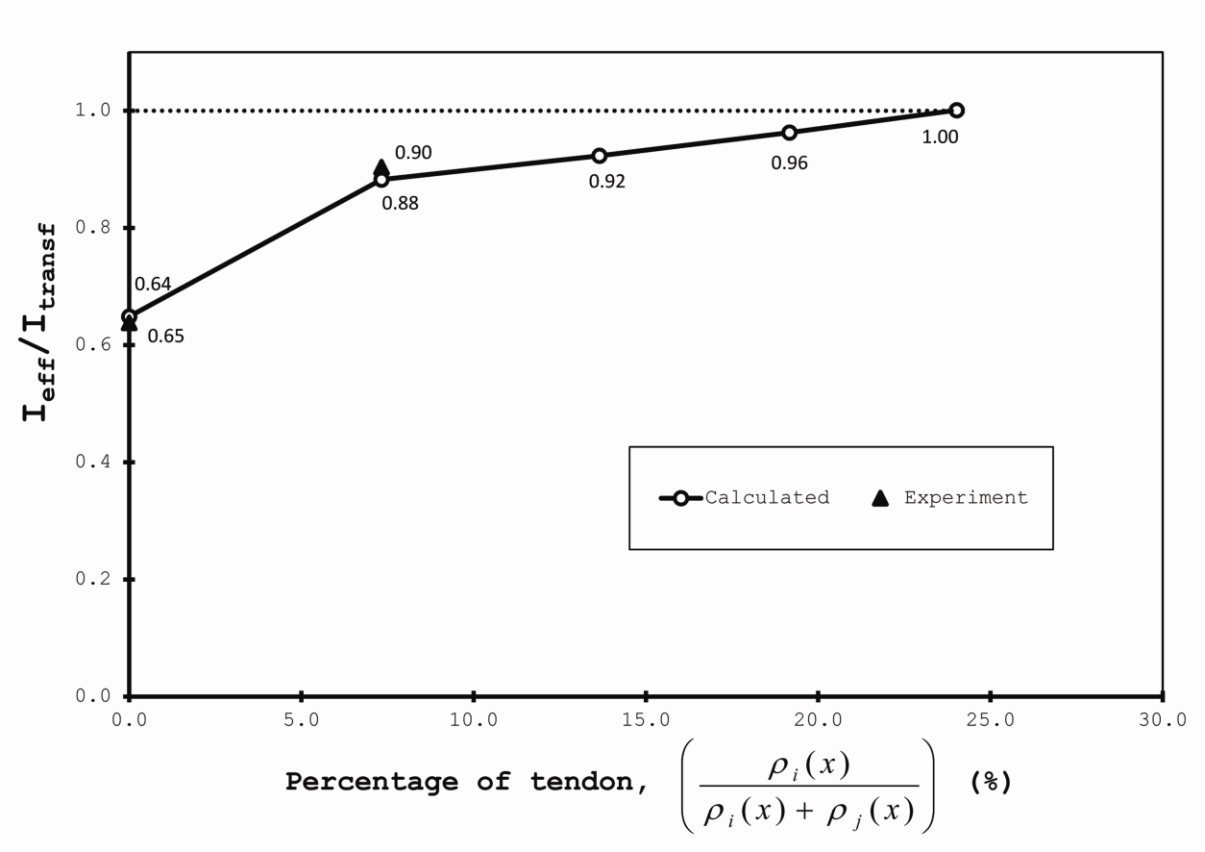

Figure 12. Effect of percentage of tendon to the effective moment of inertia

From Figure 12, the calculated results of the I_{eff} to I_{transf} ratio from the slope of the load and deflection curves are very close to the experimental results. The higher percentage of tendon improves the ratio of the effective flexural stiffness and the transformed section flexural stiffness, (I_{eff} / I_{transf}), which means that the transformed section method will give more accuracy to the approximation of the composite truss defection calculation.

Summarize the Advantages of Strengthening the Composite Truss by Post-Tensioning

From the experimental results as well as the theoretical analysis, the advantages of strengthening the composite truss by post-tensioning are presented for the general case of the post-tensioned composite truss.

Ultimate Moment Capacity

The ultimate moment capacity of a composite truss strengthened by post-tensioning can be computed from Equations (5), (6), (7) and (8);

$$M_u = T_{\max}\left\{h-\left(\frac{a}{2}\right)\right\} \tag{5}$$

$$a = \left(\frac{T_{\max}}{0.85 f_c' b}\right) \tag{6}$$

$$T_{\max} = \min\left\{\left(A_i(x)\cdot f_u + P + \Delta P\right), \sum Q_u, \left(0.85 f_c' b t_c\right)\right\} \tag{7}$$

$$\Delta P_{\max} = \frac{\left\{\left(\frac{1}{\delta P_2}\right)\sum_{i=1}^{n}\int_0^L\left(\frac{F_{i,1}(x)\delta F_{i,2}(x)}{E_i(x)A_i(x)}\right)dx\right\}}{\left[\left(\frac{1}{\delta P_2}\right)\left\{\sum_{i=1}^{n}\int_0^L\left(\frac{F_{i,2}(x)\delta F_{i,2}(x)}{E_i(x)A_i(x)}\right)dx + \sum_{j=1}^{m}\int_0^L\left(\frac{F_{j,2}(x)\delta F_{j,2}(x)}{E_j(x)A_j(x)}\right)dx\right\}\right]} \quad (8)$$

All of the additional symbols, notations and abbreviations are listed below;
M_u is the ultimate moment capacity of the post-tensioned composite truss.
T_{max} is the maximum tensile force in the bottom chord.
h is the distance between the top concrete surface to the centroid of the bottom chord member. f_c' is the concrete compressive strength of the deck slab.
f_u is the tensile strength of the truss bottom chord member.
b is the effective width of the composite truss.
ΣQ_u is the summation of the horizontal shear stud capacity between the points of maximum to the zero moment.
t_c is the concrete deck slab thickness.
$\Delta P_{\max}$ is the increase in tendon force at the ultimate stage.

Please be noted that ΔP in Equation (8) is the increase in tendon force at the time the tensile stress of the truss bottom chord member reaches the tensile strength of its material.

Ultimate Shear Capacity

The ultimate shear capacity of the post-tensioned composite truss depends on the tensile strength of the critical web members in tension and the buckling strength of the critical web members in compression. The following Equation (9) can be applied;

$$\sigma_{web} = \left[\sigma_{DL} + \sigma_{LL} + \sigma_P + \sigma_{\Delta P}\right] \leq \left(\sigma_u, \sigma_{cr}\right) \quad (9)$$

All of the additional symbols, notations and abbreviations are listed below;
σ_{web} is the web member stress in tension/compression.
σ_{DL} is the web member stress due to the dead load.
σ_{LL} is the web member stress due to the live load
σ_P is the web member stress due to the post-tensioning.
$\sigma_{\Delta P}$ is the web member stress due to the increasing of the post-tensioning from the live load.
σ_u is the ultimate tensile strength of the web member material.
σ_{cr} is the critical buckling strength of the web member.

Maximum Applicable Tendon

From the study and the experimental preparation, the maximum applicable tendon is also mentioned. The tendon prestressing force causes a compressive stress in the bottom chord of the composite truss. If the lateral bracings are provided adequately, the bottom chord stress may reach the compressive strength. The maximum prestressing force for this criterion can be calculated from Equation (10)

$$P \leq \frac{\sigma_u}{\left(\frac{1}{A_{transf}} + \frac{e \cdot y_b}{I_{transf}}\right)} \tag{10}$$

All of the additional symbols, notations and abbreviations are listed below;
σ_u is the ultimate compressive strength of the truss bottom chord member material.
A_{transf} is the transformed sectional area of the composite truss.
I_{transf} is the transformed moment of inertia of the composite truss.
e is the eccentricity from the distance from the composite truss neutral axis to the centroid of bottom chord.
y_b is the distance from the composite truss neutral axis to the bottom fiber of the steel bottom chord member.

If there is no lateral support available, the truss web members can be considered as the lateral support as refer to Benson (2009) since the truss web members welded to the top chord member which behaves like a fixed base by the anchored shear stud connectors embedded in the concrete slab. The lateral translation stiffness of the bottom chord considering the web member as the lateral bracings, K_H, is computed from Equation (11)

$$K_H = \frac{3 \cdot E_w \cdot I_w}{d_w^3} \tag{11}$$

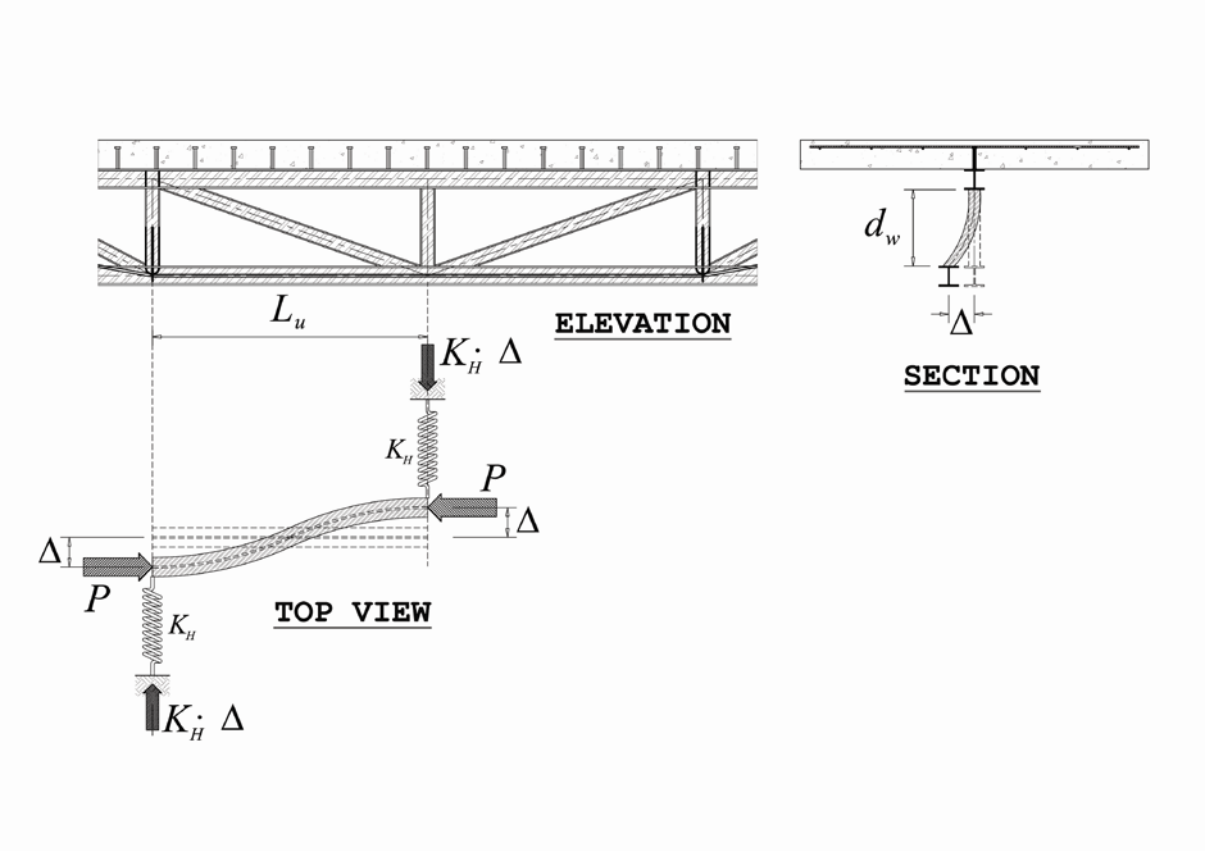

Figure 13: Loaded configuration of bottom chord under post-tensioning with web member as lateral bracing

Refer to the Figure 13, take the equilibrium condition;

$$P \cdot (2\Delta) = K_H \cdot \Delta \cdot L_u \tag{12}$$

Rearrange the equation; the maximum post-tensioned force that can be applied to the bottom chord without any buckling problem can be compute from Equation (13)

$$P \leq \frac{3 \cdot E_w \cdot I_w}{d_w^3} \left(\frac{L_u}{2} \right) \tag{13}$$

All of the additional symbols, notations and abbreviations are listed below;
E_w is the modulus of elasticity of the web member in the lateral direction.
I_w is the sectional moment of inertia of the web member in the lateral direction.
d_w is the total distance from the concrete bottom surface to the centroid of bottom chord.
L_u is the unbraced length between the two adjacent web members.

Since during prestressing, the top surface of the concrete slab is under tensile stress. The next limitation of the maximum prestressing force to prevent the concrete top surface from cracking during the prestressing is computed from Equation (14)

$$P \leq \frac{f_r \cdot n}{\left(\frac{1}{A_{transf}} + \frac{e \cdot y_t}{I_{transf}} \right)} \tag{14}$$

All of the additional symbols, notations and abbreviations are listed below;
f_r is the concrete modulus of rupture of the deck slab.
n is the modular ratio computed from the ratio of the steel elastic modulus over the concrete elastic modulus.
y_t is the distance from the composite truss neutral axis to the top fiber of the concrete deck slab.

The final limitation for the maximum tendon force is the tendon strength itself. The total internal stress from the initial jacking stress and the increasing stress from the applied ram loads must remain less than or equal to the ultimate strength of the tendon material as defined by Equation (15)

$$P + \Delta P \leq \left(f_{pu} \cdot A_j(x) \right) \tag{15}$$

All of the additional symbols, notations and abbreviations are listed below;
f_{pu} is the ultimate tensile strength of the tendon material.
$A_j(x)$ is the cross sectional area of the tendon.

The maximum post-tensioned force must satisfy Equations (9), (10), (13), (14) and (15).

Conclusions

Base on the experimental results and also the theoretical analysis, composite trusses strengthened by the external high strength tendons are believed to perform better than conventional composite trusses. With respect to this noticeably better performance, the following observations are presented:

- The additional 7.9% of the cross sectional area of the post-tensioned tendons compared to the tensile bottom chord area of the truss resulted in the 20.4% of the load carrying capacity higher than the case without post-tensioning.
- Beneficial aspects of post-tensioning are most notable for the steel trusses with concrete composite deck slab. The concrete decks provide the effective lateral support for the steel top chord under the ultimate stage and also perform rigid base for the truss web member as the lateral support for the bottom chord to prevent the lateral buckling failure under the post-tensioning stage.
- Failure mode of the post-tensioned composite truss occurs by yielding of the bottom chord while the tendon is still in the elastic range. This behavior is quite desirable as it results in a ductile failure mode with the better rotational capacity which displays detectable warning deformation indicative of impending collapse.
- Local buckling of truss member should be prevented when the prestressing level is increased. Sufficient lateral bracings for the truss members are required to apply the post-tensioning.
- Percentage of tendon improves the linearity of the load and deflection response. By applying the prestressing forces, the stiffness calculated from the transformed section method can be applied with the better accuracy for the approximate deflection prediction.
- Shear stud connectors must provide sufficient shear transfer strength especially for post-tensioned composite truss since the interface shear force is higher than in the case of ordinary composite truss.
- Summarize of the advantages of strengthening the composite truss by external post-tensioning in both the flexural strength and the shear capacity considering the amount of the post-tensioned tendons are presented as well as the limitations of the maximum tendon applicable; the compression failure of the bottom chord due to the post-tensioning, the buckling of the truss members due to the post-tensioning, the cracking of the top surface concrete slab and the tendon tensile strength itself.

Acknowledgement

The author would like to thank TRF (Thailand Research Fund) through the Royal Golden Jubilee Ph.D. Program (Grant No PHD/0257/2545) awarded to Mr. Kanokpat Chanvaivit and Prof. Dr. Ekasit Limsuwan for the Ph.D. Study in Chulalongkorn University, Thailand. The experimental study was conducted in the structural laboratory of the Department of Civil Engineering, University of New Brunswick, Fredericton, Canada with funding from NSERC which is greatly appreciated along with in kind contributions from DSI America, LaFarge and PCA.

References

[1] ACI Committee 318, *Building Code Requirements for Structural Concrete (ACI 31811) and Commentary (ACI 318R-11)*, American Concrete Institute, Michigan, United States, 2011.

[2] J.H. Ahn, C.Y Jung, and S.H. Kim, "Evaluation on structural behaviors of pre-stressed composite beams using external prestressing member," *Structural Engineering and Mechanics: An International Journal*, Vol. 34, No. 2, 2010.

[3] American Institute of Steel Construction, *Metric Load and Resistance Factor Design Specification for Structural Steel Buildings*, American Institute of Steel Construction Inc, Chicago, Illinois, United States, 2010.

[4] ASCE – ACI Joint Committee on Composite Construction, "Tentative recommendations for the design and construction of composite beams and girders for buildings," *Journal of the Structural Division ASCE*, Vol. 86, No. 12, pp. 73-92, 1960.
[5] ASCE (American Society of Civil Engineers) Task Committee on Design Criteria for Composite Structures in Steel and Concrete, "Proposed specification and commentary for composite joists and composite trusses," *Journal of Structural Engineering ASCE*, Vol. 122, No. 4, pp. 350-358, 1996.
[6] B.M. Ayyub, A. Ibrahim, and D. Schelling, "Posttensioned trusses: Analysis and design," *Journal of Structural Engineering ASCE*, Vol. 116, No. 6, pp. 1491-1505, 1990.
[7] B.M. Ayyub, and A. Ibrahim, "Posttensioned trusses: Reliability and redundancy," *Journal of Structural Engineering ASCE*, Vol. 116, No. 6, pp. 1507-1521, 1990.
[8] B.M. Ayyub, Y.G. Sohn, and H. Saadatmanesh, "Prestressed composite girders under positive moment," *Journal of Structural Engineering ASCE*, Vol. 116, No. 11, pp. 2931-2951, 1990.
[9] A. Brattland, and D.J.L. Kennedy, *Shrinkage and Flexural Tests of Two Full-Scale Composite Trusses*, Thesis (Master's), Department of Civil Engineering, University of Alberta, Canada, 1986.
[10] S. Benson, *Stability of Open Web Steel Joists Subjected to Wind Uplift*, Thesis (PhD), Department of Civil Engineering, University of New Brunswick, Canada, 2009.
[11] Canadian Institute of Steel Construction, *Handbook of Steel Construction*, Quadratone Graphics Ltd., Toronto, Ontario, Canada, 2011.
[12] S. Chen, Y. Jia, and X. Wang, "Experimental study of moment redistribution and load carrying capacity of externally prestressed continuous composite beams," *Structural Engineering and Mechanics, An International Journal*, Vol. 31, No. 5, pp. 605-619, 2009.
[13] K.B. Han, and S.K. Park, "Parametric study of truss bridges by the post-tensioning method," *Canadian Journal of Civil Engineering*, Vol. 32, pp. 420-429, 2005.
[14] P.G. Hoadley, "Behavior of prestressed composite steel beams," *Journal of the Structural Division ASCE*, Vol. 89, No. 3, pp. 21-33, 1963.
[15] S.H. Kim, C.Y. Jung, and J.H. Ahn, "Ultimate strength of composite structure with different degrees of shear connection," *Steel and Composite Structures: An International Journal*, Vol. 11, No. 5, pp. 375-390, 2011.
[16] R.E. Klingner, and J.A. Mendonca, "Shear capacity of short anchor bolts and welded studs: A litterature review," *American Concrete Institute (ACI) Journal*, Vol. 79, No. 5, pp. 339-349, 1982.
[17] D. Lam, and E. El-Lobody, "Behavior of headed stud shear connectors in composite beam," *Journal of Structural Engineering ASCE*, Vol. 131, No. 1, pp. 96-107, 2005.
[18] T. Lou, and Y. Xiang, "Numerical analysis of second-order effects of externally prestressed concrete beams," *Structural Engineering and Mechanics: An International Journal*, Vol. 35, No. 5, 2010.
[19] J. Nie, Y. Xiao, Y. Tan, and H. Wang, "Experimental studies on behavior of composite steel high-strength concrete beams," *American Concrete Institute (ACI) Structural Journal*, Vol. 101, No. 2, pp. 245-251, 2004.
[20] M. Ohsaki, and J. Zhang, "Stability conditions of prestressed pin-jointed structures," *International Journal of Non-Linear Mechanics Elsevier*, Vol. 41, pp. 1109-1117, 2006.
[21] H. Saadatmanesh, P. Albrecht, and B.M. Ayyub, "Analytical study of prestressed composite beams," *Journal of Structural Engineering ASCE*, Vol. 115, No. 9, pp. 2364-2381, 1989.
[22] H. Saadatmanesh, P. Albrecht, and B.M. Ayyub, "Experimental study of prestressed composite beams," *Journal of Structural Engineering ASCE*, Vol. 115, No. 9, pp. 2348-2363, 1989.
[23] H. Saadatmanesh, P. Albrecht, and B.M. Ayyub, "Guidelines for flexural design

of prestressed composite beams," *Journal of Structural Engineering ASCE*, Vol. 115, No. 11, pp. 2944-2961, 1989.
[24] D. Samuelson, "Composite steel joist," *Engineering Journal*, pp. 111-120, 2002.
[25] B. Uy, and S. Craine, "Static flexural behavior of externally post-tensioned steel-concrete composite beams," *Advances in Structural Engineering,* Vol. 7, No. 1, pp. 1-20, 2004.
[26] F.J. Vechio, P. Gauvreau, and K. Liu, "Modeling of unbonded post-tensioned concrete beams critical in shear," *ACI Structural Journal,* Vol. 103, No. 1, pp. 57-64, 2006.